# Dynamic Analyses of a Tube in a Fluid

I.-W. Yu, W. Vanburen
*Westinghouse Electric Corporation, R & D Center, 1310 Beulah Road, Pittsburgh, Pennsylvania 15235, U.S.A.*

SUMMARY

In dynamic analyses of structural response in fluids, the added mass (hydrodynamic or virtual mass) method is perhaps the simplest approach which accounts for the dynamic interaction between a structure and its surrounding fluid. The added mass method is often applicable to a class of practical problems when the structural vibration is of small amplitude and low frequency, and the fluid motion can be described as an ideal fluid flow. In this paper a finite element procedure for performing an added mass fluid-structure analysis is presented by using a submerged four-tube array as an example. The hydrodynamic mass matrix for the tube array is generated using the substructural technique of a finite element code. By combining the substructural hydrodynamic mass with the structure, many dynamic events such as normal modes, shock spectrum, and time history analyses are carried out. Several interesting structural responses in fluids are discussed.

In normal mode analysis the tube array in the fluid shows a significant drop in natural frequencies compared to that of the in-vacuo frequencies. The in-fluid frequencies are clustered around several bands and the frequencies within each band are often closely spaced. The shock response analysis shows the modes which actively participate in the motion are not necessarily those nearest to the fundamental frequency. A pluck test (free vibration) is performed for the demonstration of a time history analysis. Due to the closely spaced nature of the frequencies within each band, the response of the free vibration shows a strong interference between modes and the phenomenon of beating is clearly observed.

In order for these analyses to serve as benchmark problems for different finite element computer codes, complete details of the problem data as well as the important results are presented in the paper.

## 1. Introduction

In considering structural vibrations in fluid, the added mass (hydrodynamic or virtual mass [1]) approach provides a simple method of representing the fluid-structure interaction. This simple approach is often found practical in problems when the structural vibration is of small amplitude and long wave length, and the fluid motion can be described as an ideal fluid flow (i.e., inviscid and incompressible). The finite element analysis of an added mass fluid-structure interaction problem requires the generation of a hydrodynamic mass in addition to the structure. Applying the substructural technique of a finite element code, the hydrodynamic mass of a structure can easily be generated using a procedure developed by Yu [2]. Using a submerged four-tube array as an example, the computational procedure for the added mass fluid-structure interaction under normal mode, shock spectrum, and time history are analyzed. Numerical results which characterize the tube response in fluids are discussed.

## 2. Governing Equations

For the added mass fluid-structure interaction analyses, it is convenient to represent the fluid field by its dynamic pressure, p, which satisfies the Laplace equation

$$\nabla^2 p = 0 \tag{1}$$

The boundary conditions on the free surface and the fluid-structure interface are

$$p = 0 \tag{2}$$

$$\partial p/\partial n = -\rho\, \ddot{\delta}_n \tag{3}$$

Here n is the interface normal (outward from the fluid), $\rho$ is the fluid density, and $\ddot{\delta}_n$ is the structural acceleration in the n-direction. In terms of the fluid pressure and the structural displacement, the finite element equations representing the free vibration of the fluid-structure system can be expressed by [2]

$$[M]\,\{\ddot{\delta}\} + [K]\,\{\delta\} = [L]\,\{p\} \tag{4}$$

$$[H]\,\{p\} = -\rho\,[L]^T\{\ddot{\delta}\} \tag{5}$$

where $\{\delta\}$ and $\{\ddot{\delta}\}$ are the structural displacement and acceleration vectors; [M] and [K] are the mass and stiffness matrices; $\{p\}$ is the fluid pressure vector; [H] is the fluid matrix and [L] is the fluid-structure interface (area) matrix. Upon the substitution of (5) into (4) the added mass fluid-structure system is described by the following equation:

$$([M] + [M^*])\,\{\ddot{\delta}\} + [K]\,\{\delta\} = \{0\} \tag{6}$$

where [M*] is the symmetrical hydrodynamic mass matrix determined by

$$[M^*] = \rho\,[L][H]^{-1}[L]^T \tag{7}$$

## 3. Determination of the Hydrodynamic Mass

As described in reference [2] the determination of the hydrodynamic mass requires only the consideration of the fluid region and the fluid-structure interface. The relations between the fluid pressure and the structural acceleration at the interface are

$$\left[\begin{array}{c|c} 0 & -L \\ \hline -L^T & -H/\rho \end{array}\right] \left\{\begin{array}{c} \ddot{\delta} \\ \hline p \end{array}\right\} = \left\{\begin{array}{c} f \\ \hline 0 \end{array}\right\} \tag{8}$$

Using the substructuring technique by condensing out all the pressures, the following equations can be obtained

$$(\rho[L][H]^{-1}[L]^T)\ \{\ddot{\delta}\} = \{f\} \tag{9}$$

The coefficient matrix of the above equation is the desired hydrodynamic mass. It is also clear that the force vector {f} can be interpreted as the added fluid inertial force to the structure. In forming the system matrix (8) using the WECAN [3] general purpose finite element code, the matrix $-[H]/\rho$ can be formulated using heat conduction elements by redefining the thermal conductivity to be equal to $-1/\rho$. The interface area matrix $-[L]$ is formulated using special interface elements [2].

The procedure requires that the fluid matrix [H] be invertible; this is possible only if the fluid region has a free surface. For situations where a fluid region is entirely enclosed by a structure, the fluid matrix [H] is singular and the substructuring procedure requires a slight modification. Instead of eliminating all the pressures, it is necessary to retain one pressure degree-of-freedom for each enclosed fluid region. Letting these retained pressures be denoted by {p*}, the condensed substructural system has the following expression

$$\left[\begin{array}{c|c} M^*_{\delta\delta} & M^T_{p\delta} \\ \hline M_{p\delta} & 0 \end{array}\right] \left\{\begin{array}{c} \ddot{\delta} \\ \hline p^* \end{array}\right\} = \left\{\begin{array}{c} f \\ \hline 0 \end{array}\right\} \tag{10}$$

where the submatrix $[M^*_{\delta\delta}]$ is the desired hydrodynamic mass and the $p^*_i$ are the Lagrange multipliers associated with the constraint equations

$$[M_{p\delta}]\ \{\ddot{\delta}\} = \{0\} \tag{11}$$

The above equations are the direct result of

$$[M_{p\delta}]\ \{\delta\} = \{0\} \tag{12}$$

which ensure the incompressibility of the enclosed fluid regions [2].

## 4. Numerical Examples for a Submerged Four-Tube Array

Consider a square array of four tubes submerged in a rigid square container filled with water, as shown in Fig. 1. The four tubes are fixed to the container at the bottom and are free at the top. For the geometrical data and the mechanical properties shown in Table 1, the response of the tube array under different dynamic events is analyzed.

### 4.1 Hydrodynamic Mass for the Four-Tube Array

By assuming that the flow around the tube is essentially two-dimensional, it is sufficient to consider only the cross-section of the tube array and to determine the hydrodynamic mass for a unit depth of the fluid. Due to the symmetry of the problem only a 45°-segment of the fluid region is modelled as shown in Fig. 2. To formulate the system eq. (8), the pressure field in the fluid region is modelled by 6-node isoparametric triangular elements, and the fluid-structure interfaces (at the tube and container) are modelled by 3-node isoparametric interface elements [2,3]. Using the 45°-segment as a substructure the complete system model can be generated.

By assuming that the tube cross-section has only negligible deformation during vibration, each cross-section of the tube moves as a rigid body, as does the outside container (i.e., rigid bodies 1 through 5 as shown in Fig. 2). A substructuring run was performed for the complete model by retaining the x- and y-accelerations of the five bodies and one fluid pressure as the substructural degrees-of-freedom. The final condensed substructural matrix is an 11 x 11 matrix and contained in it is the 10 x 10 sub-matrix for the hydro-

dynamic mass as shown in Table 2. The finite element results show that the substructural matrix coefficients for the pressure degree-of-freedom are nearly zero (i.e., $10^{-8}$ of the diagonals). This implies that the incompressibility of the fluid is satisfied automatically if the five structures are moving in a rigid body manner.

By examining the hydrodynamic mass, all the physical symmetries, such as the symmetry in x and y and the permutational symmetry on the four tubes, are satisfied by the matrix. Also, by letting the five bodies move in the x-direction with unit acceleration, the total added mass is computed to be 2.126 kg/m which agrees exactly with the mass of the fluid between the five bodies.

### 4.2 Normal Mode Analysis

To determine the normal modes of the submerged four-tube array, each tube is modelled by 5 thin-walled pipe elements and the outside container is assumed to be fixed. The hydrodynamic mass is incorporated into the model as a substructure [3] and there are 6 substructural mass matrices at the nodal levels of the finite element model. Each substructure has a scalar multiplication on the hydrodynamic mass matrix to account for the depth of the fluid it represents.

The natural frequencies of the first 16 modes determined for the four-tube array both in-vacuo and in-fluid are shown in Table 3. The first 8 modes are cantilever modes with an in-vacuo frequency of 17.10 Hz and in-fluid frequencies ranging from 11.96 to 15.32 Hz. Patterns of the tube motion for the first 8 modes are grouped according to their symmetry about the x and y axes as shown in Fig. 3. The second group of modes (9-16) are similar to the first 8 modes except that the tubes are deformed in the second cantilever mode.

### 4.3 Shock Spectrum Analysis

By assuming that the container is subjected to an excitation (or shock) which can be expressed in terms of a shock spectrum as shown in Fig. 4, the maximum tube response can be determined using the shock spectrum method.

Since the dynamic event is symmetric about x and antisymmetric about y, only modes possessing the (S,A) symmetry participated in the motion. The results show that the dynamic response is dominated almost entirely by modes 4 and 5. The spectral displacements are shown in Table 4. If the maximum tube displacement is estimated by taking the square-root-of-the-sum-of-the-squares (SRSS) of the spectral displacements for modes 4 and 5, the free end of the tube displaces a maximum of .07522 and .01499 cm in the x and y directions, respectively.

### 4.4 Time History Analysis

Consider the same finite element model used for the normal mode and shock spectrum analyses and assume that the system is undamped and that the outside container is fixed. Initially, let the free end of tube 1 be displaced in the x-direction by 0.1 cm and hold the tube stationary. At time t=0 the tube is released and the motion of the tube array during the time interval t=0∿1 sec is to be determined. The problem can be analyzed using the transient dynamic analysis capability of the WECAN code [3] by choosing the Houbolt time integration operator with a time increment $\Delta t$=0.002 sec. Figs. 5.1 through 5.4 are the displacement histories for tubes 1 through 4, respectively. Examination of these figures shows that the tubes are vibrating in the frequency band of the first 8 cantilever modes. Since these frequencies are relatively close, the interference of two modes generates the

phenomenon known as beating. As a result, beats are clearly shown in the motion of the four tubes. Comparison of Figs. 5.2 and 5.4 shows that the plucking of tube 1 in x generates a higher vibration amplitude for tube 4 than for tube 2, which is facing the incoming motion.

## 5. Conclusions

A simple numerical exercise has been carried out for the analysis of a submerged tube array under different dynamic events. Although the main purpose of this paper is to provide benchmark problems to industrial practioners who are using finite element computer codes in solving their design problems, the results generated from each example may also interest some research workers in the area of fluid-elastic vibration. Phenomena such as the patterns of mode shapes and the closeness of the natural frequencies often generate certain unique dynamic responses which are difficult to predict.

## References


[1] Lamb, H., "On the Vibrations of an Elastic Plate in Contact with Water," Proc. Roy. Soc. (London), Ser. A, Vol. 98, pp. 205-216, 1921.

[2] Yu, I.-W., "Determination of Hydrodynamic Mass Using a General Purpose Finite Element Structural Code," ASME Paper No. 80-C2/PVP-117, Century 2 PVP Conference, San Francisco, Aug. 1980.

[3] WECAN-Westinghouse Electric Computer ANalysis User's Manual, Edited by Filstrup, A. W., Westinghouse R&D Center, Pittsburgh, PA, March 30, 1981.


TABLE 1 - PROBLEM DATA

| Geometry | | Mechanical Properties | |
|---|---|---|---|
| Container size | $b = 5.715$ cm | Fluid density | $\rho = 10^3$ kg/m$^3$ |
| Tube spacing | $a = 2.54$ cm | Tubes: Young's modulus | $E = 2.034 \times 10^8$ kPa |
| Tube length | $\ell = 1.016$ m | Density | $\rho_s = 7853$ kg/m$^3$ |
| Tube outside radius | $R = 0.9525$ cm | | |
| Tube wall thickness | $t = 0.15875$ cm | | |

TABLE 2 - HYDRODYNAMIC MASS (kg/m) FOR THE FIVE BODY SYSTEM

| | AX(1) | AY(1) | AX(2) | AY(2) | AX(3) | AY(3) | AX(4) | AY(4) | AX(5) | AY(5) |
|---|---|---|---|---|---|---|---|---|---|---|
| AX(1) | .48239 | .01164 | -.04435 | -.01945 | .01828 | -.04530 | .16186 | .01945 | -.90318 | .03366 |
| AY(1) | .01164 | .48239 | .01945 | .16186 | -.04530 | .01828 | -.01945 | -.04435 | .03366 | -.90318 |
| AX(2) | -.04435 | .01945 | .48239 | -.01164 | .16186 | -.01945 | .01828 | .04530 | -.90318 | -.03366 |
| AY(2) | -.01945 | .16186 | -.01164 | .48239 | .01945 | -.04435 | .04530 | .01828 | -.03366 | -.90318 |
| AX(3) | .01828 | -.04530 | .16186 | .01945 | .48239 | .01164 | -.04435 | -.01945 | -.90318 | .03366 |
| AY(3) | -.04530 | .01828 | -.01945 | -.04435 | .01164 | .48239 | .01945 | .16186 | .03366 | -.90318 |
| AX(4) | .16186 | -.01945 | .01828 | .04530 | -.04435 | .01945 | .48239 | -.01164 | -.90318 | -.03366 |
| AY(4) | .01945 | -.04435 | .04530 | .01828 | -.01945 | .16186 | -.01164 | .48239 | -.03366 | -.90318 |
| AX(5) | -.90318 | .03366 | -.90318 | -.03366 | -.90318 | .03366 | -.90318 | -.03366 | 6.87880 | -.00000 |
| AY(5) | .03366 | -.90318 | -.03366 | -.90318 | .03366 | -.90318 | -.03366 | -.90318 | -.00000 | 6.87881 |

* AX(I) AND AY(I) ARE X AND Y ACCELERATIONS FOR BODY I .

TABLE 3 - NATURAL FREQUENCIES FOR THE FOUR-TUBE ARRAY

| Mode No. | Frequencies (Hz) In-Vacuo | Frequencies (Hz) In-Fluid | Mode No. | Frequencies (Hz) In-Vacuo | Frequencies (Hz) In-Fluid |
|---|---|---|---|---|---|
| 1 | 17.10 | 11.96 | 9 | 106.94 | 73.13 |
| 2 | 17.10 | 12.13 | 10 | 106.94 | 74.17 |
| 3 | 17.10 | 12.26 | 11 | 106.94 | 75.05 |
| 4 | 17.10 | 12.26 | 12 | 106.94 | 75.05 |
| 5 | 17.10 | 13.63 | 13 | 106.94 | 83.86 |
| 6 | 17.10 | 13.63 | 14 | 106.94 | 83.86 |
| 7 | 17.10 | 13.80 | 15 | 106.94 | 84.94 |
| 8 | 17.10 | 15.32 | 16 | 106.94 | 94.96 |

TABLE 4 - SPECTRAL DISPLACEMENT FOR MODES 4 & 5

| Tube | Spect. Displ. Mode 4 u (cm) | Spect. Displ. Mode 4 v (cm) | Spect. Displ. Mode 5 u (cm) | Spect. Displ. Mode 5 v (cm) |
|---|---|---|---|---|
| Free End | .75503E-1 | .10600E-1 | .14878E-2 | .10598E-1 |
| . | .54709E-1 | .76808E-2 | .10785E-2 | .76820E-2 |
| . | .34738E-1 | .48770E-2 | .68500E-3 | .48793E-2 |
| . | .17306E-1 | .24296E-2 | .34135E-3 | .24315E-2 |
| . | .48099E-2 | .67528E-3 | .94897E-4 | .67596E-3 |
| Fixed End | .0 | .0 | .0 | .0 |

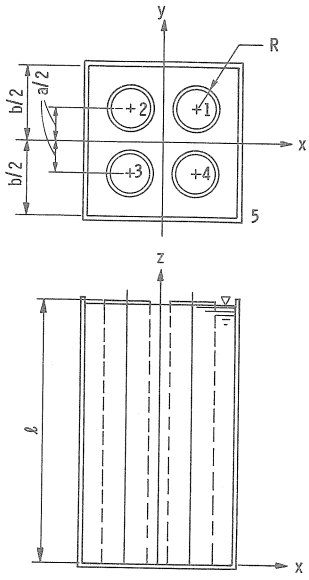


Fig. 1—Four tubes submerged in a container

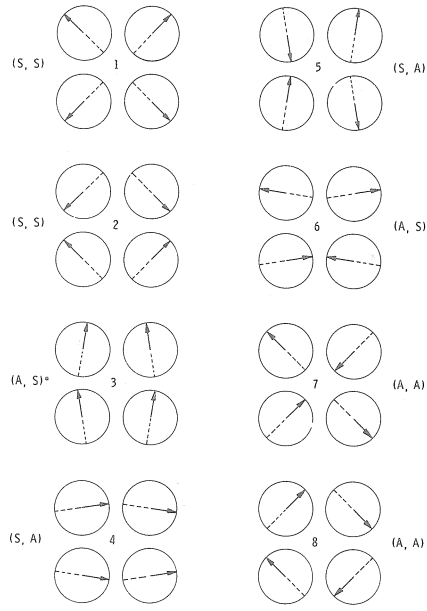


* (A, S) = Antisymmetry about x-axis and symmetry about y-axis

Fig. 3—Patterns of in-fluid tube displacement for the first 8 modes

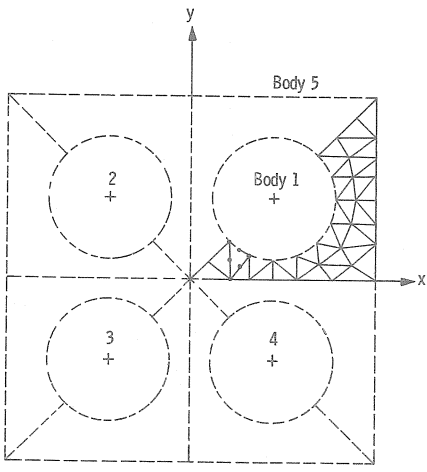


Fig. 2—Finite element model for a 45°-segment

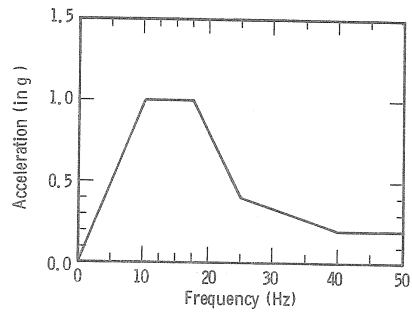


Fig. 4—Shock spectrum

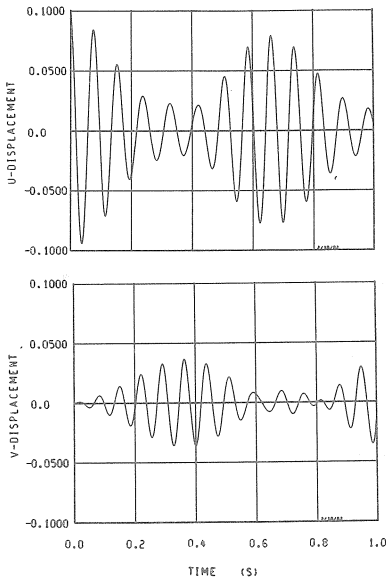


Fig. 5.1—Vibration of tube 1

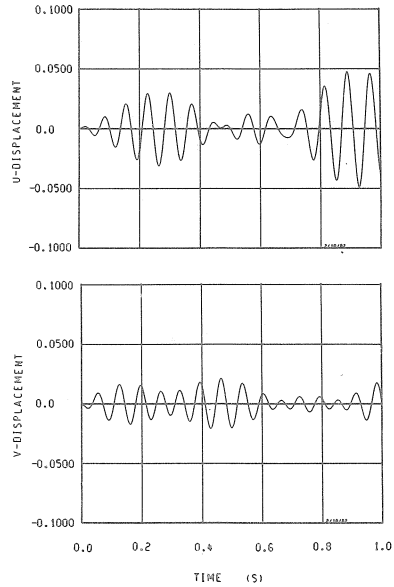


Fig. 5.3—Vibration of tube 3

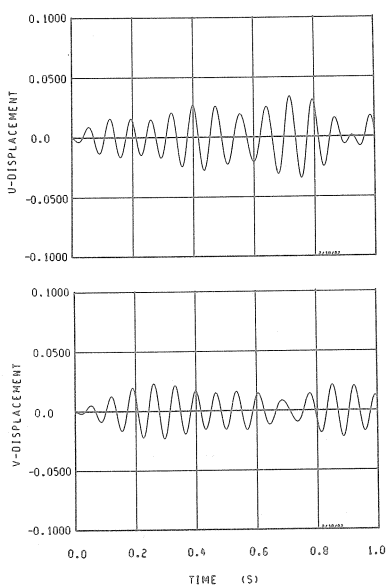


Fig. 5.2—Vibration of tube 2

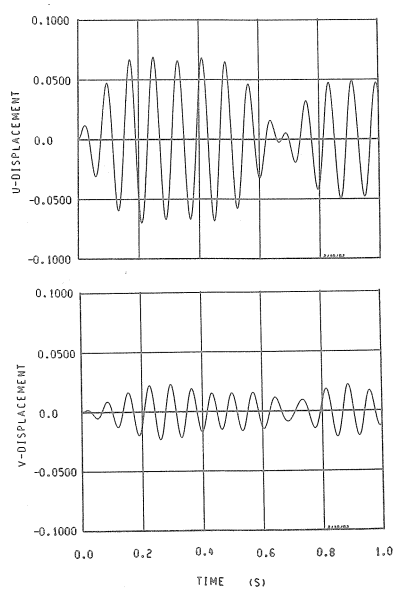


Fig. 5.4—Vibration of tube 4